

1 **Geochemical characterisation of northern Norwegian fjord surface** 2 **sediments: a baseline for further paleo-environmental** 3 **investigations**

4 *Johan C. Faust*^{1,2,*}, *Thomas Scheiber*^{1,3}, *Karl Fabian*^{1,4}, *Christoph Vogt*⁵ and *Jochen Knies*^{1,4}

5 ¹ Geological Survey of Norway, Leiv Eirikssons vei 39, 7040 Trondheim, Norway

6 ² School of Earth and Environment, University of Leeds, Leeds LS2 9JT, United Kingdom

7 ³ Western Norway University of Applied Sciences, Sogndal, Norway

8 ⁴ CAGE - Centre for Arctic Gas Hydrate, Environment and Climate, Department of Geology, UiT the Arctic University of
9 Norway, 9037 Tromsø, Norway

10 ⁵ Central Laboratory for Crystallography and Applied Material Science (ZEKAM) & Crystallography, Geosciences, University
11 of Bremen, 28359 Bremen, Klagenfurter Strasse 2-4, Germany

13 **Abstract**

14 Norwegian fjord sediments are promising archives for very high resolution records of past
15 environmental changes. Recent investigations of the modern depositional environment
16 within fjords revealed that the accurate quantification of the inputs, sources, and
17 sedimentary preservation of organic and inorganic material is crucial to decipher long term
18 past climate signals in the sedimentary record of a certain fjord. Here, we investigate the
19 elemental composition, bulk mineral assemblage and grain size distribution of forty-one
20 surface sediment samples from a northern Norwegian fjord system. We reveal modern
21 geochemical and sedimentological processes that occur within the Vestfjord, Ofotfjord and
22 Tysfjord. Our results indicate a very heterogeneous sediment supply and intricate
23 sedimentation processes. We propose that this is related to the complex fjord bathymetry, a
24 low hydrodynamic energy environment, differences in the hinterland bedrock composition
25 and a relatively small drainage area causing a rather diffuse freshwater inflow. Moreover,
26 we show that marine carbonate productivity is the main calcite and Ca source in all three
27 fjords.

28 **1 Introduction**

29 Sediments accumulating in fjords have the potential to be one of the best high-resolution
30 archives of climate and local environmental changes (Howe et al., 2010). High
31 sedimentation together with the possibility to quantify the fjord's hydrological cycle

32 (freshwater input and marine water exchange) offer an excellent opportunity for studying
33 land-ocean interactions and can provide ultra-high-resolution records of local responses to
34 short-term climate variability (Faust et al., 2016; Forwick and Vorren, 2007; Hald and
35 Korsun, 2008; Howe et al., 2010; Husum and Hald, 2004; Kristensen et al., 2004; Mikalsen et
36 al., 2001; Paetzel and Dale, 2010; Syvitski, 1989).

37 In general, it is assumed that changes in precipitation and temperature alter the
38 constitution of fluvial sediment flux, generated by weathering and erosion of bedrock and
39 soils, from land towards ocean basins (e.g. Govin et al., 2012; Lamy et al., 2001; White and
40 Blum, 1995). However, a detailed knowledge of the controlling transport mechanisms of the
41 particle supply is required to explore the relationship between terrigenous input and
42 changes in environmental conditions (Zabel et al., 2001). Sediment characteristics,
43 accumulation and distribution vary with climate, seafloor topography, basin geometry, size
44 of the drainage area, oceanographic regime, and distance to river outlets (e.g. Syvitski et al.,
45 1987). Thus, identifying the provenance of the sediment components is the key factor to
46 determine and reconstruct (1) sea-level changes, (2) hinterland weathering processes, (3)
47 climate variability and (4) anthropogenic influences. For this reason numerous studies have
48 focused on the contribution of organic carbon (e.g. Goñi et al., 1997; Knies and Martinez,
49 2009; Sargent et al., 1983; Stein and MacDonald, 2004; Winkelmann and Knies, 2005) and
50 trace elements (e.g. Calvert et al., 1993; Cho et al., 1999; Govin et al., 2012; Hayes, 1993;
51 Hirst, 1962; Karageorgis et al., 2005; Kim et al., 1999; Mil-Homens et al., 2014; Pe-Piper et
52 al., 2008) in continental shelf sediments.

53 Fjords comprise a substantial part of the coastal environments and are important sites for
54 carbon burial due to their high inorganic and organic sedimentation rates (Hedges et al.,
55 1997; Knies, 2005; Knudson et al., 2011; Ludwig et al., 1996; Raymond and Bauer, 2001;
56 Sepúlveda et al., 2011; Smith et al., 2015; St-Onge and Hillaire-Marcel, 2001; Syvitski et al.,
57 1987) but only a very few studies exist using surface sediments to investigate modern fjord
58 environmental settings. Studies from fjords in Chile (Bertrand et al., 2012; Sepúlveda et al.,
59 2011; Silva et al., 2011), New Zealand (Hinojosa et al., 2014; Knudson et al., 2011; Smith et
60 al., 2015), east Greenland (Andrews and Vogt, 2014) and Svalbard (Winkelmann and Knies,
61 2005) reported a significant influence of freshwater inflow on their geochemical
62 composition and suggest a common decreasing gradient of terrigenous-derived organic- and
63 inorganic material from the inner fjords towards the open ocean. In contrast to these

64 findings, Munoz and Wellner (2016) found terrigenous deposits to occur predominantly in
65 the outer bay of an Antarctic fjord. This indicates that the processes controlling the supply
66 and composition of the inorganic sediment fraction of fjords sediments may vary from fjord
67 to fjord. More investigations of fjord sediments are therefore required to recognize and
68 better understand these differences.

69 Overall, little is known about seasonal and bathymetry-related changes in sedimentation of
70 particulate material in Norwegian fjords. Recent investigations of surface sediment samples
71 from the Trondheimsfjord, mid-Norway, revealed that not only does the input of
72 terrigenous material vary in proximity to their source but also geochemical composition of
73 the material changes with regard to the hinterland geology (Faust et al., 2014b). Moreover,
74 as shown by Faust et al. (2016; 2014a) a detailed study of the modern environmental fjord
75 setting provides fundamental knowledge necessary to interpret climatic signals in long term
76 fjord sediment sequences.

77 Similar to the Trondheimsfjord, the regional climate of Vestfjord, Ofotfjord and Tysfjord in
78 northern Norway is strongly influenced by the relatively warm northward flowing North
79 Atlantic Current (NAC) and the atmospheric circulation pattern is dominated by the North
80 Atlantic Oscillation (NAO) (Hurrell, 1995). Thus, sediments from these fjords may contain
81 valuable information about regional past climate changes caused by NAO and NAC
82 variability. Moreover, although the study area was an important pathway for ice-sheet
83 drainage during the late Weichselian (Ottesen et al., 2005), ice-sheet dynamics during the
84 Younger Dryas period in the Vestfjord, Ofotfjord and Tysfjord area is still under debate
85 (Bergstrøm et al., 2005; Fløistad et al., 2009; Knies et al., 2007; Rasmussen, 1984). Hence,
86 the identification of geochemical or mineralogical provenance proxies could help to better
87 understand the deglaciation history in this area. The hinterland geology, bathymetry and
88 oceanography of the Vestfjord, Ofotfjord and Tysfjord are overall similar to the intensively
89 investigated Trondheimsfjord in mid Norway. Our hypothesis is that these similarities of the
90 environmental settings make the Vestfjord, Ofotfjord and Tysfjord sediments a promising
91 archive for paleo-environmental studies. To test our hypothesis, we investigate
92 geochemical, mineralogical and sedimentological data obtained from forty-one surface
93 sediment samples from the Vestfjord, Ofotfjord and Tysfjord in northern Norway (Fig. 1).
94 Our goal is to acquire a better understanding of the modern processes that control the

95 supply and composition of the inorganic sediment fraction of the fjords. We discuss the
96 general trends within these deposits, assess how local variations affect sediment
97 distribution and provide implications for paleo-environmental interpretations.

98 **2 Regional setting**

99 The Vestfjord, Ofotfjord and Tysfjord are the three main fjords of a fjord system between
100 the Norwegian mainland and the Lofoten archipelago in northern Norway (Fig. 1). With a
101 length of about 180 km and its cone shape the Vestfjord is an "*atypical*" fjord and has
102 characteristics more similar to a coastal bay (Fig. 2, Mitchelson-Jacob and Sundby, 2001).
103 The fjord becomes shallower and widens from about 15 km at its junction with the Ofotfjord
104 and Tysfjord in the NE to about 70 km at the entrance in the SW. Moreover, the boundaries
105 between the deeper Vestfjord basin and its shallower coastal areas on the SE and NW sides
106 are marked by up to 300 m high side-edges (Fig. 1). This is interpreted to be the result of
107 enhanced glacial erosion of the downfaulted Vestfjord basin as the Vestfjord functioned as a
108 major ice-sheet drainage route during the last glacial period (Ottesen et al., 2005). The
109 Ofotfjord and Tysfjord morphologies are, as is typical for fjords, characterised by narrow
110 trenches, steep slopes and an entrance sill with varying water depths of 140–350 m (Fløistad
111 et al., 2009). The fjord basins on both sides of the sill are elongated and remarkably deep
112 (500–725 m, Fig 1).

113 The total drainage area of the three fjords spans about 7,100 km² (Fig. 2) and is marked by a
114 relatively sparse vegetation cover and an alpine landscape. Mountains in this region are
115 frequently higher than 1000 m and several small glaciers are present in the drainage area of
116 the Tysfjord and Ofotfjord (Fig. 2). February air temperatures (monthly average) are around
117 0°C at the coast and minus 5 to minus 10°C in the hinterland. During August, hinterland air
118 temperature (monthly average) rises to about 14–15°C and around 11°C at the coast.
119 Precipitation varies strongly over short distance with topography (500–2000 mm/a) and is
120 highest during summer/autumn and lowest in spring (The Norwegian Meteorological
121 Institute (met.no)). No large river exists and the runoff is generally low during winter when
122 inland water is frozen and high during summer due to snow melt and rainfall. On average
123 two thirds of the annual runoff occurs from June to August (Mitchelson-Jacob and Sundby,
124 2001). For more detailed information of the topography, rivers and further hydrological

125 information of the drainage area, we refer to the Norwegian Mapping Authorities
126 (<http://kart.statkart.no>) and the Norwegian Water Resources and Energy Directorate
127 (<http://atlas.nve.no>).

128 The oceanography of the fjord system is driven locally by wind and bathymetry and
129 regionally by tides and the adjacent North Atlantic and Norwegian Coastal Current systems
130 (Furnes and Sundby, 1981; Mitchelson-Jacob and Sundby, 2001). Due to the seasonal
131 variation of freshwater supply, temperature and salinity of the surface water layer (up to
132 150 m deep) vary between 2–4°C and 33–34 (PSU) during winter and about 14°C and 28
133 (PSU) during summer. The surface layer overlies an Atlantic water layer, which has constant
134 temperatures and salinity of 6.5–7°C and 34.7–35 (PSU) throughout the year. There are no
135 observations of anoxic conditions in the fjords (Gitmark et al., 2014). The general surface
136 circulation can be described by inflowing Atlantic water along the southeast side (mainland)
137 and an outflow current along the northwest side (Lofoten) with cyclonic circulation in
138 between (Mitchelson-Jacob and Sundby, 2001). Yet, this major current regime is strongly
139 affected by the dominant wind direction. SW winds reverse the flow direction and may
140 induce upwelling on the Lofoten side and downwelling on the mainland side (Fig. 2).
141 Additionally, the SW winds cause an enhanced flow of upper water masses into the
142 Vestfjord, Ofotfjord and Tysfjord, which presses the underlying Atlantic water out of the
143 fjords (Furnes and Sundby, 1981). NE winds cause the opposite effect. They force the upper
144 water layer out of the fjords which results in an inflow of Atlantic water and may induce
145 downwelling on the Lofoten side and upwelling on the mainland side (Fig. 2).

146 The bedrock geology in the drainage areas of the Vestfjord, Ofotfjord and Tysfjord can be
147 subdivided into Precambrian basement units and overlying Caledonian nappes (Fig. 2). The
148 basement is largely composed of Paleoproterozoic plutonic rocks of the anorthosite-
149 mangerite-charnockite-granite (AMCG) suite intruding older metamorphic rocks (Corfu,
150 2004). The Caledonian nappes predominantly contain metamorphosed Ordovician-Silurian
151 sediments such as micaschist, metasandstone and subordinate marble (Andresen and
152 Steltenpohl, 1994; Corfu et al., 2014).

153 3 Methods and Data

154 3.1 *Fjord surface sediments: sampling and preparation*

155 In June 2014, forty-one surface sediment samples were collected at water depth between
156 59 and 634 m across the Vestfjord, Ofotfjord and Tysfjord (67°40'N, 13°00'E, 68°40'N,
157 17°40'E) (Fig. 1 and ES-1). In general, sediments are mainly transported by rivers into fjords
158 and the main controlling factors of their distribution are the bathymetry of the fjord and
159 oceanography. Therefore, sampling locations were selected based on water depth,
160 distance to river inlets and coastal water inflow in order to cover the entire sedimentary
161 regime of the three fjords. Moreover, each sampling site has been investigated using a
162 TOPAS (Topographic Parametric Sonar) prior to coring to avoid turbidites or other large
163 disturbance in the sediment structure. The first two centimetres of two 5.5 cm wide
164 multicores were sampled at every station aboard the research vessel "FF Seisma"
165 (Geological Survey of Norway) and stored in plastic bags at minus 18°C. Prior to analyses, all
166 samples were freeze-dried and, except for grain size measurements, homogenised through
167 grinding.

168 3.2 *Bulk elemental geochemistry and grain size analyses*

169 Four combined analytical methods were used to quantify major and trace elements at the
170 ALS Geochemistry Laboratories in Loughrea, Ireland. A subsample of 0.9 g was added to 9 g
171 of Lithium Borate Flux, well mixed and fused between 1050 to 1100°C. A molten disc was
172 prepared from the resulting melt and analysed for the major elements (Al, Ca, Fe, K, Mg,
173 Mn, Na, P, Si, Ti) by X-Ray Fluorescence Spectroscopy (XRF). For the analysis of Ba, Ce, Cr, Cs,
174 Dy, Er, Eu, Ga, Gd, Hf, Ho, La, Lu, Nb, Nd, Pr, Rb, Sm, Sn, Sr, Ta, Tb, Th, Tm, U, V, W, Y, Yb and
175 Zr a 0.2 g subsample was added to 0.9 g of lithium metaborate flux and fused at 1000°C. The
176 resulting melt was cooled and dissolved in 100 ml 4% HNO₃/2% HCl and the solution was
177 subsequently analysed by inductively coupled plasma mass spectrometry (ICP-MS).
178 Determination of Ag, Cd, Co, Cu, Li, Mo, Ni, Pb, Sc and Zn was performed by inductively
179 coupled plasma atomic emission spectroscopy (ICP-AES) following a four-acid total digestion
180 method. 250 mg of each sample was heated (200°C) in a mixture of H₂O-HF-HClO₄-HNO₃
181 (2:2:1:1) and the residue was dissolved in hydrochloric acid (50%) and analysed.

182 The determination of the grain size distribution was performed by laser diffraction using a
183 Coulter LS 13320 instrument at the Geological Survey of Norway. The analysis was carried
184 out on material within a particle diameter range of 0.4–2000 μm and the results are
185 presented as cumulative volume percentage. Prior to the grain size analyses, sediment
186 samples were decarbonated using 10% (vol.) hydrochloric acid (HCl), organic matter was
187 removed using hydrogen peroxide (H_2O_2) and to prevent particles becoming charged and
188 agglomerated all samples were treated with 5% sodium pyrophosphate ($\text{Na}_4\text{P}_2\text{O}_7 \cdot 10\text{H}_2\text{O}$,
189 Merck PA). Samples were then placed in an ultrasonic bath until analysis. We assume that
190 biogenic silica has a negligible effect on the grain size measurement because (I) the biogenic
191 silica content in North Atlantic sediments is generally very low (e.g. Schlüter and Sauter,
192 2000), (II) biogenic silica content in Trondheimsfjord sediments (Mid-Norway) was found to
193 be very small (Faust et al., 2014b) and (III) our XRD analysis reveal only traces of amorphous
194 silica (<0.3%) in just six samples.

195 3.3 *Bulk mineral assemblage*

196 Bulk mineral assemblages were measured via X-ray diffraction (XRD) using a Bruker D8
197 Advance diffractometer with $\text{Cu K}\alpha$ radiation and a Lynxeye XE detector at the Geological
198 Survey of Norway, Trondheim, Norway. XRD scans were carried out for 3–75° 2θ and a step
199 size of 0.02°. Signal acquisition time was 1 s per step. The optical system was equipped with
200 soller slits (2.5°) and fixed divergence and antiscatter slits (0.6 mm). Quantification of the
201 mineral content was carried out with Quantitative Phase-Analysis with X-ray Powder
202 Diffraction (QUAX) (details are given in Vogt et al., 2002). Bulk mineral assemblages from
203 station 29 are missing due to insufficient sediment material.

204 4 Results and Discussion

205 4.1 Grain size and mineral assemblages

206 Grain size distribution in marine sediments is generally a good indicator for sediment
207 erosion, transport and deposition and mineral assemblages. Changes in sediment grain size
208 may also provide information about the sediment origin. The bulk mineral assemblages of
209 the Vestfjord, Ofotfjord and Tysfjord sediments consist mainly of phyllosilicates (23%) and

210 plagioclase (22%) followed by quartz (14%), calcite (13%) and potassium feldspars (9%) (ES-1
211 and ES-2). However, the mineral content varies considerably from sample to sample (7%–
212 50% phyllosilicates, 2%–36% plagioclase, 1%–31% quartz, 1%–51% calcite). Moreover,
213 sediments are generally fine-grained (<63 μm) in the inner part of the Ofotfjord (station 1–3,
214 5) and in the deepest part of the Vestfjord (station 17, 39, 30) (Fig. 3). Samples from the
215 inner part of the Tysfjord (station 23–26), the sill (station 14, 15) and partly from the shelf
216 areas of the Vestfjord (station 38, 41, 28) are more coarse-grained (>125 μm). On average,
217 all surface sediments samples consist mainly of the 2–63 μm (average 74%) and 63–125 μm
218 (average 15%) fractions. However, the amount of the 2–63 μm and 63–125 μm fraction
219 varies between 27%–93% and 1%–40%, respectively (Fig. 3). Moreover, the mean grain size
220 distribution resembles the 2–63 μm fraction ($r = 0.95$, $n = 41$) and all other fractions are on
221 average $\leq 5\%$.

222 The variable mineral- and grain size distribution in the surface sediments indicates a very
223 heterogeneous sediment supply and complex sedimentation processes. In general, it is
224 assumed that the distribution of sediments within a fjord is largely controlled by its
225 bathymetry, depth and hydrographic regime (Howe et al., 2010). However, in our study area
226 neither grain size nor specific mineral assemblages show any characteristic spatial
227 distribution pattern (Fig. 3 and ES-2). Exceptions are the clay fraction (<2 μm) as well as
228 phyllosilicates, expandable- and mixed layer clays, which reveal statistical relevant Pearson
229 correlation coefficients with water depth ($r = 0.5$ – 0.7 , $p < 0.01$, $n = 40$, ES-1). This
230 relationship is in accordance with the general assumption that the deepest parts of a fjord
231 are in general the lowest energy environments (Syvitski, 1989) and therefore, favour the
232 settlement of fine-grained material. Due to longer transport distances, we would further
233 expect the portion of the fine-grained material to increase with increasing distance from the
234 coast. However, grain size and quartz content in the Vestfjord sediments increase towards
235 the open ocean (Station 30–33). We assume that this indicates that stronger bottom water
236 currents caused winnowing and sediment redistribution in the outer part of the fjord.

237 The local mineral and grain size distribution shows a complex distribution pattern which can
238 be explained by the physiographic setting of the study area. Considerable changes in land
239 topography cause irregular precipitation over very short distances and the relatively small
240 drainage area of the three fjords prevent longer river systems to form. Hence, freshwater

241 inflow is often rather diffuse and we assume that these environmental conditions may cause
242 irregular erosion and a very inhomogeneous sediment supply from each drainage area,
243 which results in strong variations of the sediment composition even over very short
244 distances.

245 **4.2 Geochemistry**

246 The inorganic geochemical composition of the surface sediments from the Vestfjord,
247 Ofotfjord and Tysfjord reveals a very heterogeneous pattern. Simple and multivariate
248 statistical data analysis failed to provide a better understanding of the association of the
249 analysed parameters or the spatial distribution pattern. We found that an individual
250 examination of the geochemical characteristics of each fjord is required because in our
251 study area the element distribution is not necessarily related to a specific grain size fraction
252 or mineral. As such, in the following, we discuss each fjord individually and depict
253 similarities and differences between the analysed parameters. We focus our discussion
254 mainly on the elements of Al, Si, Hf, Fe, Ti, and Zr because most of these elements are
255 frequently used as indicators of terrestrial sediment supply in sediment core studies (e.g.
256 Bertrand et al., 2012; Brendryen et al., 2015; Faust et al., 2014a; Wehrmann et al., 2014;
257 Zabel et al., 2001). Moreover, to avoid dilution and grain size effects, we discuss the spatial
258 distribution of these elements in the fjords as Al-based ratios (Bertrand et al., 2012; Faust et
259 al., 2014b; Loring, 1990).

260 *4.2.1 Ofotfjord*

261 *Linkage between terrigenous elements, grain size and water depth*

262 In the Ofotfjord, Si correlates strongly with Hf and Zr and these elements are the only
263 elements which are positively related to quartz ($r = 0.7\text{--}0.8$; $p < 0.01$, $n = 11$, ES-1).
264 Moreover, they are related to the $>63\ \mu\text{m}$ grain size fraction and show a clear negative
265 correlation with the water content of the samples, water depth and with other terrigenous
266 elements like Al, Mg, Fe, K, Ti, and Ni (ES-1). These elements (Al, Mg, Fe, K, Ti, Ni) correlate
267 positively with the water content of the sediment samples and the $<63\ \mu\text{m}$ grain size
268 fraction. Additionally, they have a strong positive relationship to kaolinite and the sum of
269 phyllosilicates (ES-1). The spatial distribution of Si/Al in the Ofotfjord (Fig. 4) shows that the

270 fine-grained material, which is rich in Al and clay minerals, settles in the middle and deeper
271 part of the fjord. Closer to the shore and at the entrance sill, sediments show higher
272 percentages of coarse-grained material, which are enriched in quartz and Si (Fig. 3 and ES-
273 2). This finding is in accordance with the typical sediment distribution pattern in fjords,
274 where coarser and heavier sediment components are usually deposited at the shore and in
275 river estuaries and the grain size decreases with depth (Holtedahl, 1975; Skei, 1983). The
276 higher amounts of Si and quartz together with the larger grain sizes at the entrance sill (Fig.
277 3 and ES-2) are probably related to winnowing caused by higher bottom current velocity.

278 *4.2.2 Tysfjord*

279 Narrow and long fjord arms, deep basins (up to 725 m) and large changes in depth over very
280 short distances (Fig. 1) result in complicated geochemical and mineralogical signatures in
281 the Tysfjord. Moreover, we note that the interpretation of the Tysfjord sediments
282 composition is biased by the fact that sediment samples from the deepest part of the fjord
283 are missing and that the number of sediment samples (ten) is relatively low to obtain
284 reliable statistical analysis.

285 *4.2.2.1 Connection between terrigenous elements and water depth*

286 Similar to the Ofotfjord, Si, Hf, Zr and Ti are negative correlated with the water content of
287 the sample, water depth and the <63 μm grain size fraction (ES-1). Thus, Si concentrations
288 are higher close to the shore and in shallower areas. The strong relationship between Si and
289 the water depth explains the varying Si/Al values in the inner most fjord arms and over very
290 short distances (Fig. 4 and ES-2). For example, station 23 and 25 are both located in the
291 inner arms of the Tysfjord but station 23, which is at 120 m water depth shows much higher
292 Si/Al values (3.9) than station 25 (2.7), which is at 444 m water depth (Fig. 4). Also the
293 neighbouring stations 19 and 20 show very different Si/Al values (4 and 3.2, respectively)
294 likely due to a change in water depth of 322 meters (Fig. 4). In accordance with the
295 environmental setting in Patagonian fjords (Bertrand et al., 2012) these results suggest that
296 the distribution of Si, Zr, Hf and also Ti in the surface sediments of the Tysfjord (and
297 Ofotfjord) are controlled by their association to heavy and coarse-grained minerals such as
298 quartz, zircon, amphibole, pyroxene and rutile. Furthermore, Bertrand et al. (2012) showed
299 that Zr/Al and Ti/Al are sensitive to changes in the energy of the terrestrial supply to the

300 fjords. In a low energy system, values are highest in deltaic and proximal fjord environments
301 of the tributaries. Moreover, Hinojosa et al. (2014) investigated several New Zealand fjords
302 and concluded that differences in down-fjord geochemical gradients were related the
303 presence or absence of a major river outlet in the inner fjord and amount of freshwater
304 inflow. Thus in the Tysfjord, the clear relationship of Si, Hf, Zr and Ti with the water depth
305 and the separation of fine and coarse-grained material even on a relatively short distance
306 (e.g. station 19 and 20), indicates that the energy of the hydrodynamic system in the
307 Tysfjord is relatively low. This is likely due to the small drainage area and the lack of large
308 rivers entering the fjord.

309 4.2.2.2 *Origin of potassium*

310 Similar as in Ofot- and Vestfjord sediments, K has a strong, positive correlation with the
311 <63 μm grain size fraction, the mixed and expandable clay minerals and Na (ES-1). However,
312 in contrast to both other fjords, K shows no significant positive correlation to any other
313 element or mineral. The relationship of K to the fine-grained material and the lack of
314 correlation with almost any other element and mineral phase suggest that the analysed K
315 originates potentially from a mixture of different (clay) minerals and may be a sign of an
316 individual K source in the hinterland. The spatial distribution of the grain-size independent
317 K/Al ratio reveals a clear inside-outside trend (Fig. 5) with highest values at the entrance of
318 the fjord, which points to a possible K source in the middle to outer Tysfjord. Potassium is
319 generally not associated with a specific mineral in sediments. Although, K-feldspar, kaolinite
320 and illite are known as possible K sources in marine sediments (Martinez et al., 1999;
321 Shimmiel, 1992; Yarincik et al., 2000), these minerals do not correlate with K in the
322 Tysfjord sediments (ES-1). Parts of the Precambrian basement in the mid-Tysfjord drainage
323 area consist of biotite and K-feldspar rich gneisses (Andresen and Tull, 1986; Karlsen, 2000;
324 Müller, 2011) and complementary airborne radiometric data indicate Precambrian rocks in
325 northern Norway to be enriched in K (Nasuti et al., 2015). The Caledonian rocks in our study
326 area are enriched in muscovite. However, since K does not show a significant correlation
327 with the muscovite content ($r = -0.3$, $p > 0.1$, $n = 10$) in the Tysfjord sediments the
328 Caledonian rocks can probably be excluded as potential K source. Thus, we conclude that
329 Precambrian rocks are the main source of K in the Tysfjord sediments and we suggest that
330 temporal changes of K/Al can be applied as an indicator of the variable supply of sediments

331 from the Precambrian rocks. Hence, K/Al in sedimentary records from the Tysfjord may be
332 used to investigate past changes in terrestrial input and, thus, reconstruct variable
333 freshwater inflow, weathering and glacial erosion.

334 4.2.3 Vestfjord

335 *Two different sedimentary regimes*

336 Similar to the sediments from Ofot- and Tysfjord, Si shows a positive correlation with Hf, Zr
337 and quartz in the Vestfjord (ES-1). However, unlike the other fjords there is also a strong
338 positive affiliation of Si to Al ($r = 0.9$, $p < 0.01$, $n = 20$) and to other terrigenous elements
339 such as Ti, K, Fe (ES-1). These elements (Ti, K, Fe), however, show only a very weak
340 correlation with quartz, but they are related to the phyllosilicates, chlorite, illite and micas
341 (ES-1). A closer investigation of the relationship between quartz, Fe and Si in the surface
342 sediments from the Vestfjord reveals two different sedimentary regimes. Considering all
343 samples from the Vestfjord, quartz is strongly related to Si ($r = 0.8$, $p < 0.01$, $n = 19$) but not
344 to Fe ($r = 0.2$, $p > 0.1$, $n = 19$) and both, Fe and Si are related to the sum of illites and micas
345 ($r = 0.7$, $p < 0.01$, $n = 19$) (Fig. 6). Together with Al, K, Mg, and Ti, Fe is strongly related to the
346 water depth of the sample ($r = 0.9$, $p < 0.01$, $n = 20$, Fig. 6), and the highest Fe
347 concentrations ($>3.5\%$) are found in the middle of the fjord along an inside-outside trend
348 (stations 17; 30–33; 39; 42; 43, Fig. 1). By examining the samples from the deeper and the
349 shallower areas (shelf and sill) separately, we found that Fe and quartz are positive
350 correlated on the shelf areas ($r = 0.6$, $p = 0.05$, $n = 11$, Fig. 6) but negatively correlated in the
351 deeper and outer fjord basins ($r = -0.9$, $p < 0.01$, $n = 8$, Fig. 6). This division by the two
352 territories is also present in many other geochemical and mineralogical parameters in the
353 Vestfjord surface sediment samples. For example, Al versus plagioclase reveals a clear
354 positive correlation ($r = 0.9$, $p < 0.01$, $n = 11$) for the shelf and sill sediment samples and a
355 clear negative correlation ($r = -0.8$, $p < 0.05$, $n = 8$) for the samples from the deeper
356 Vestfjord basin (Fig. 6). Moreover, Al versus the sum of phyllosilicates (Fig. 6) shows an
357 increase of the Pearson correlation coefficient from $r = 0.4$ at the shallow parts to $r = 0.9$ in
358 the deeper fjord areas. Sediments at the Vestfjord shelf and sill area contain higher amounts
359 of coarse-grained material (Fig. 3) and the positive correlation, for example between Al and
360 plagioclase, and Si and quartz, shows that the sediment material is relatively fresh and of

361 local origin. The samples from the deeper basins are rich in fine-grained material (Fig. 3),
362 and Al and Si are negative correlated to plagioclase and quartz and positively correlated to
363 clay minerals. Due to the relatively small catchment area of the Vestfjord, about 90% of the
364 freshwater inflow originates from the adjacent fjords in the east (Mitchelson-Jacob and
365 Sundby, 2001; Sundby, 1982). Thus, the fine-grained sediments in the deep basin of the
366 Vestfjord may be transported over longer distances and may derive also from the Ofot- and
367 Tysfjord. Indications of sediment transport from these two fjords into the Vestfjord are also
368 found in the distribution of biotite and illite. Compared to the other fjords, the Vestfjord is
369 enriched in illite (Fig. 7) which shows no relationship to the water depth and is present in
370 the shallow and the deep parts of the fjord. Yet, apart from one sample (station 15; 0.6%),
371 biotite is only found in the deep areas of the Vestfjord (station 17, 30–33, 39, 42, 43, (ES-1)).
372 This indicates that biotite does not originate from the Vestfjord drainage area but it
373 originates from the Ofotfjord or the biotite-rich Tysfjord area (Fig. 7). Thus, the surface
374 sediments forming the deep Vestfjord basin probably contain a sediment mixture of all
375 adjacent fjords.

376 To summarize, we found a very heterogeneous spatial distribution pattern of most analysed
377 elements. In general, this can be explained by the complex fjord bathymetry with large
378 changes in water depth over very short distances, a low hydrodynamic energy environment
379 and a relatively small drainage area causing a rather diffuse freshwater inflow. Similar to the
380 sediments from Ofot- and Tysfjord, elements associated with coarser and heavier sediment
381 components (Si, Hf, Zr) are enriched at the shallower areas and higher values of elements
382 often associated with the fine grain material (Al, Fe, K) are found in the deeper fjord basins.
383 Potassium in the Tysfjord reveals a solitary behaviour which points to an individual K source
384 in the hinterland. This source is probably biotite and K-rich Precambrian rocks enclosing the
385 middle to outer Tysfjord. Similar as in the Tysfjord and Ofotfjord, Vestfjord sediments at the
386 shelf are relatively fresh and of local origin. But in contrast to the two other fjords the
387 surface sediments forming the deep Vestfjord basin probably contain a sediment mixture of
388 all adjacent fjords. The differences of the elemental distribution in the Vestfjord are caused
389 by a different origin of the sediment material and differences in the grain size/mineralogical
390 association of certain elements. Hence, the distribution of a certain element in fjord
391 sediments is not necessarily related to a specific grain size fraction or mineral.

392 **4.3 Terrigenous provenance proxies: biotite, muscovite and illite**

393 Most phyllosilicates are detrital and their distribution in shelf sediments depends largely on
394 the diversity of geology and weathering processes of the contributing source areas in the
395 hinterland (e.g. Petschick et al., 1996; Velde, 1995). We found that the Ofotfjord sediments
396 are enriched in muscovite, the Tysfjord in biotite and the Vestfjord in illite (Fig. 7). The
397 different mineral assemblages of the three fjords may reflect differences in the bedrock
398 composition in the drainage areas. Muscovite is very common in the Caledonian rocks
399 surrounding the Ofotfjord. On the contrary, Precambrian rocks in the drainage areas of the
400 Vest- and Tysfjord are relatively poor in muscovite. Moreover, biotite-rich gneisses in the
401 Tysfjord drainage area (Andresen and Tull, 1986; Karlsen, 2000; Müller, 2011) probably
402 contribute to the elevated biotite concentrations in the Tysfjord (Fig. 7). However, we note
403 that biotite, muscovite and illite are very common minerals and typically found in marine
404 sediments in boreal regions where weathering is largely physically controlled (e.g. Vogt and
405 Knies, 2009). It is, therefore, very challenging to identify a particular source of these
406 minerals in the hinterland. Nevertheless, the occurrence of large amounts of biotite and
407 chlorite, which are usually unstable under hydrolysis (Petschick et al., 1996; Wilson, 2004) in
408 the fjord sediments, and the low concentrations of secondary clay minerals such as kaolinite
409 (2–3%) and smectite (0–2%), indicate that the fjord sediments are relatively fresh and of
410 very local origin. We suggest that these findings are probably related to the relatively small
411 drainage areas of the three fjords. Therefore, distance and time between erosion and
412 sedimentation is short and additionally the temperate climate in northern Norway favour
413 physical- over chemical weathering.

414 **4.4 Ca and calcite: marine productivity proxies**

415 Their strong relationship to marine productivity and, thus, water temperature, salinity,
416 nutrient supply and degree of ice coverage make Ca, calcite and CaCO_3 very appropriate
417 proxies to reconstruct climate and environmental changes (e.g. Schneider et al., 2006). The
418 CaCO_3 content in surface sediments usually reflects the modern surface water
419 oceanography and was, for example, successfully applied as a paleoceanographic tool to
420 reconstruct northern Hemisphere glacial/interglacial cycles (e.g. Bond et al., 1992;
421 Ruddiman and McIntyre, 1981; Zamelczyk et al., 2014). Furthermore, Faust et al. (2016)

422 recently revealed that Ca/Si and CaCO₃ in fjord sediments can provide detailed
423 reconstructions of atmospheric circulation changes. In this study, we attempt to identify the
424 controlling factors of the Ca and CaCO₃ distribution in the Vestfjord, Ofotfjord and Tysfjord
425 to assess their future applicability as paleo-environmental proxies in these three fjords.

426 Ca anti-correlates to all other elements or minerals other than calcite, aragonite and Sr ($r \geq$
427 0.9 , $p < 0.01$, $n = 40$) in all three fjords. As elemental ratios are insensitive to dilution effects,
428 in the following we also focus on the Ca/Al distribution which shows a strong correlation
429 with Ca and calcite ($r \geq 0.9$, $p < 0.01$, $n = 40$).

430 Ca/Al in the Tys- and Ofotfjord sediments shows a clear inside-outside trend and highest
431 values are found at the entrance of each fjord and in their deepest areas (Fig. 8). Moreover,
432 calcite is present in all samples, but aragonite is only found in station 8, 13, 27 and 25 (ES-1
433 and 2). This is probably related to the occurrence of cold water corals which have been
434 found during the sampling procedure and are known to grow at and around the entrance sill
435 (Fossa et al., 2002 and references therein). Samples close to the marble formation in the
436 hinterland of the Ofot- and Tysfjord (Fig. 2) contain lowest Ca/Al concentrations in the
437 entire study area (Fig. 8 and ES-2). This indicates that the marble rocks in the fjord drainage
438 areas do not have a significant impact on the Ca/Al distribution. We assume that either the
439 terrigenous carbonates are dissolved during weathering or the marine carbonate input is so
440 much larger than the carbonate signal from the marble rocks that the terrigenous
441 carbonates are heavily diluted and are therefore barely discernible. An indication for the
442 dissolution of the dolomite rich marble during erosion is the strong association of Mg with
443 the water content of the sample, Na and NaCl in the Ofotfjord samples ($r \geq 0.9$, $p < 0.01$, $n =$
444 11 , ES-1). Mg and NaCl may be precipitated from the seawater during the freeze drying of
445 the samples prior to the geochemical analysis. As Mg shows this relationship only in the
446 Ofotfjord, this may indicate that the Ofotfjord water column is relatively enriched in Mg due
447 to the weathering of dolomite-rich marble in the drainage area. The Vestfjord and especially
448 the adjacent shelf areas are well known to be areas of high marine productivity, probably
449 sustained by nutrient-rich coastal waters and upwelling along the steep side-edges of the
450 Vestfjord (Espinasse et al., 2016; Furnes and Sundby, 1981; Sundby and Solemdal, 1984).
451 The highest Ca/Al values of the entire study area were found along the shallow coastal areas
452 on the north-western and the south-eastern fjord margins (Fig. 8). In accordance with this

453 finding, high concentrations of calcite (up to 51%) in these areas are related to large
454 numbers of shell and coral fragments in the sediment samples.

455 In accordance with findings from the Trondheimsfjord in mid-Norway and in northern
456 Chilean fjords (Bertrand et al., 2012; Faust et al., 2014b), the strong positive correlation
457 between Ca and calcite ($r = 0.96$, $p < 0.01$, $n = 40$) and a strong negative correlation ($r \leq -0.8$,
458 $p < 0.01$, $n = 40$) to any terrigenous element (as e.g. Al, Fe, Ti and Si) indicates marine
459 carbonate productivity to be the main calcite and Ca source in all three fjords. However, we
460 note that to confirm this assumption it is necessary to investigate the organic components
461 (such as C_{org} and $\delta^{13}C_{org}$) of the sediments samples to distinguish the marine and terrigenous
462 origin of Ca (Faust, 2014; Knies et al., 2003). Nevertheless, the increase in Ca/Al from the
463 inside towards the entrance of the Ofot- and Tysfjord fjords (Fig. 8) and the high values
464 along the upwelling areas in the Vestfjord are most likely caused by enhanced primary
465 productivity due to the inflow of Atlantic water. These findings express that Ca/Al is a well-
466 suited proxy for changes in carbonate marine productivity versus terrigenous sediment
467 supply and may serve as indicator for changes in the inflow of Atlantic waters versus river
468 discharge, nutrient supply and sea surface temperature changes.

469 **5 Conclusion**

470 The inorganic geochemical composition of Vestfjord, Ofotfjord and Tysfjord sediments in
471 northern Norway reveals that, as in many other fjords, Ca/Al and calcite are good indicators
472 for marine carbonate productivity versus terrigenous sediment supply. However, the
473 distribution patterns of the mineral assemblages, grain size and the elemental composition
474 are overall complex and variations on very short distances are large which indicates a very
475 heterogeneous sediment supply. Besides the Ca/Al proxy for the inflow of north Atlantic
476 water and river discharge, the geochemical signatures in the three fjords are very different
477 to the Trondheimsfjord in mid Norway. Moreover, even though the hinterland sediment
478 source areas of the three investigated fjords are relatively similar in terms of bedrock type
479 and drainage area size, our results indicate that differences in bathymetry and the
480 hydrodynamic energy can cause considerably different sedimentary regimes for each
481 Norwegian fjord. Thus, to identify the modern sedimentological and environmental setting,

482 it is important to examine each fjord basin separately. Furthermore, different erosion and
483 transport systems in the hinterland of each fjord may be responsible for the diverse
484 distribution pattern of the investigated parameters presented here. To evaluate this, further
485 investigations of the onshore sediment transport and bedrock weathering processes are
486 necessary. This will also help to better identify the sources of biotite, muscovite and illite of
487 the three fjords, as well as the origin of the K anomaly in Tysfjord sediments.

488 ***Acknowledgments***

489 We thank the crew of the RV Seisma for their professional support during our expedition. Further we
490 would like to express our gratitude to Anne Nordtømme, Clea Elisabeth Fabian and Wieslawa Koziel
491 for their help with the laboratory work. For their interest, stimulating discussions, and many useful
492 comments we thank our colleagues Roelant van der Lelij, Ola Fredin, Giulio Viola, Annina Margreth
493 and Allyson Tessin. This study was conducted under the auspices of the BASE project, a research
494 initiative at the NGU funded by Maersk Oil, Lundin Petroleum, Det Norske Oljeselskap, Wintershall
495 and the NGU. J.K. is supported by the Research Council of Norway (NRC grant 223259).

496 **Appendix**

497 Electronic supplementary data associated with this article (ES-1 (Tab. S1–S6) and ES-2 (Fig. S1–S6))
498 can be found in the online version.

499

500 References

- 501 Andresen, A., Steltenpohl, M.G., 1994. Evidence for ophiolite obduction, terrane accretion and
502 polyorogenic evolution of the north Scandinavian Caledonides. *Tectonophysics* 231, 59-70.
- 503 Andresen, A., Tull, F.J., 1986. Age and tectonic setting of the Tysfjord gneiss granite, Efyord, North
504 Norway. *Norsk Geol Tidsskr* 66, 69-80.
- 505 Andrews, J.T., Vogt, C., 2014. Source to sink: Statistical identification of regional variations in the
506 mineralogy of surface sediments in the western Nordic Seas (58°N–75°N; 10°W–40°W). *Mar Geol*
507 357, 151-162.
- 508 Bergstrøm, B., Olsen, L., Sveian, H., 2005. The Tromso-Lyngen glacier readvance (early Younger
509 Dryas) at Hinnoya-Ofofjorden, northern Norway: a reassessment. *Norges Geologiske Undersøkelse*
510 *Bulletin* 445, 73.
- 511 Bertrand, S., Huguen, K.A., Sepulveda, J., Pantoja, S., 2012. Geochemistry of surface sediments from
512 the fjords of Northern Chilean Patagonia (44-47°S): Spatial variability and implications for
513 paleoclimate reconstructions. *Geochim Cosmochim Acta* 76, 125-146.
- 514 Bond, G., Heinrich, H., Broecker, W., Labeyrie, L., Mcmanus, J., Andrews, J., Huon, S., Jantschik, R.,
515 Clasen, S., Simet, C., Tedesco, K., Klas, M., Bonani, G., Ivy, S., 1992. Evidence for Massive Discharges
516 of Icebergs into the North-Atlantic Ocean during the Last Glacial Period. *Nature* 360, 245-249.
- 517 Brendryen, J., Haflidason, H., Rise, L., Chand, S., Vanneste, M., Longva, O., L'Heureux, J.S., Forsberg,
518 C.F., 2015. Ice sheet dynamics on the Lofoten–Vesterålen shelf, north Norway, from Late MIS-3 to
519 Heinrich Stadial 1. *Quaternary Sci Rev* 119, 136-156.
- 520 Calvert, S.E., Pedersen, T.F., Thunell, R.C., 1993. Geochemistry of the surface sediments of the Sulu
521 and South China Seas. *Mar Geol* 114, 207-231.
- 522 Cho, Y.-G., Lee, C.-B., Choi, M.-S., 1999. Geochemistry of surface sediments off the southern and
523 western coasts of Korea. *Mar Geol* 159, 111-129.
- 524 Corfu, F., 2004. U–Pb Age, Setting and Tectonic Significance of the Anorthosite–Mangerite–
525 Charnockite–Granite Suite, Lofoten–Vesterålen, Norway. *Journal of Petrology* 45, 1799-1819.
- 526 Corfu, F., Andersen, T.B., Gasser, D., 2014. The Scandinavian Caledonides: main features, conceptual
527 advances and critical questions. *Geological Society, London, Special Publications* 390, 9-43.
- 528 Espinasse, B., Basedow, S.L., Tverberg, V., Hattermann, T., Eiane, K., 2016. A major Calanus
529 finmarchicus overwintering population inside a deep fjord in northern Norway: implications for cod
530 larvae recruitment success. *J Plankton Res* 38, 604-609.
- 531 Faust, J.C., 2014. Environmental response to past and recent climate variability in the
532 Trondheimsfjord region, central Norway : a multiproxy geochemical approach. The Arctic University
533 of Norway, Tromsø.
- 534 Faust, J.C., Fabian, K., Milzer, G., Giraudeau, J., Knies, J., 2016. Norwegian fjord sediments reveal
535 NAO related winter temperature and precipitation changes of the past 2800 years. *Earth Planet Sc*
536 *Lett* 435, 84-93.
- 537 Faust, J.C., Knies, J., Milzer, G., Giraudeau, J., 2014a. Terrigenous input to a fjord in central Norway
538 records the environmental response to the North Atlantic Oscillation over the past 50 years. *The*
539 *Holocene*.
- 540 Faust, J.C., Knies, J., Slagstad, T., Vogt, C., Milzer, G., Giraudeau, J., 2014b. Geochemical composition
541 of Trondheimsfjord surface sediments: Sources and spatial variability of marine and terrigenous
542 components. *Cont Shelf Res* 88, 61-71.
- 543 Fløistad, K.R., Laberg, J.S., Vorren, T.O., 2009. Morphology of Younger Dryas subglacial and ice-
544 proximal submarine landforms, inner Vestfjorden, northern Norway. *Boreas* 38, 610-619.
- 545 Forwick, M., Vorren, T.O., 2007. Holocene mass-transport activity and climate in outer Isfjorden,
546 Spitsbergen: marine and subsurface evidence. *Holocene* 17, 707-716.
- 547 Fossa, J.H., Mortensen, P.B., Furevik, D.M., 2002. The deep-water coral *Lophelia pertusa* in
548 Norwegian waters: distribution and fishery impacts. *Hydrobiologia* 471, 1-12.

549 Furnes, G., Sundby, S., 1981. Upwelling and wind induced circulation in Vestfjorden, in: Sætre, R.,
550 Mork, M. (Eds.), *The Norwegian Coastal Current, Proceedings from the Norwegian Coastal Current*
551 *Symposium, Geilo*, pp. 9-12.

552 Gitmark, J.K., Ledang, A.B., Trannum, H.C., Johnsen, T.M., 2014. Marin overvåking Nordland 2013,
553 *Undersøkelser av hydrografi, bløtbunnsfauna og hardbunnsorganismer i 6 fjorder i Nordland.*,
554 *Rapport 6638-2014. Norsk institutt for vannforskning.*

555 Goñi, M.A., Ruttenberg, K.C., Eglinton, T.I., 1997. Sources and contribution of terrigenous organic
556 carbon to surface sediments in the Gulf of Mexico. *Nature* 389, 275-278.

557 Govin, A., Holzwarth, U., Heslop, D., Ford Keeling, L., Zabel, M., Mulitza, S., Collins, J.A., Chiessi, C.M.,
558 2012. Distribution of major elements in Atlantic surface sediments (36°N–49°S): Imprint of
559 terrigenous input and continental weathering. *Geochem Geophys Geosy* 13.

560 Hald, M., Korsun, S., 2008. The 8200 cal. yr BP event reflected in the Arctic fjord, Van Mijenfjorden,
561 Svalbard. *The Holocene* 18, 981-990.

562 Hayes, J.M., 1993. Factors controlling ¹³C contents of sedimentary organic compounds: Principles
563 and evidence. *Mar Geol* 113, 111-125.

564 Hedges, J.I., Keil, R.G., Benner, R., 1997. What happens to terrestrial organic matter in the ocean?
565 *Organic Geochemistry* 27, 195-212.

566 Hinojosa, J.L., Moy, C.M., Stirling, C.H., Wilson, G.S., Eglinton, T.I., 2014. Carbon cycling and burial in
567 New Zealand's fjords. *Geochem Geophys Geosy* 15, 4047-4063.

568 Hirst, D.M., 1962. The geochemistry of modern sediments from the Gulf of Paria—II The location and
569 distribution of trace elements. *Geochim Cosmochim Acta* 26, 1147-1187.

570 Holtedahl, H., 1975. The geology of the Hardangerfjord, West Norway. *NGU Publikasjon* 323, 87.

571 Howe, J.A., Austin, W.E.N., Forwick, M., Paetzel, M., Harland, R., Cage, A.G., 2010. Fjord systems and
572 archives: a review. *Geological Society, London, Special Publications* 344, 5-15.

573 Hurrell, J.W., 1995. Decadal Trends in the North Atlantic Oscillation - Regional Temperatures and
574 Precipitation. *Science* 269, 676-679.

575 Husum, K., Hald, M., 2004. A continuous marine record 8000-1600 cal. yr BP from the
576 Malangenfjord, north Norway: foraminiferal and isotopic evidence. *Holocene* 14, 877-887.

577 Karageorgis, A.P., Anagnostou, C.L., Kaberi, H., 2005. Geochemistry and mineralogy of the NW
578 Aegean Sea surface sediments: implications for river runoff and anthropogenic impact. *Appl*
579 *Geochem* 20, 69-88.

580 Karlsen, T.A., 2000. Economic potential of potassic feldspar-rich gneisses in Tysfjord/Hamarøy,
581 northern Norway. *Norges geologiske undersøkelse Bulletin* 436, 129-135.

582 Kim, G., Yang, H.S., Church, T.M., 1999. Geochemistry of alkaline earth elements (Mg, Ca, Sr, Ba) in
583 the surface sediments of the Yellow Sea. *Chem Geol* 153, 1-10.

584 Knies, J., 2005. Climate-induced changes in sedimentary regimes for organic matter supply on the
585 continental shelf off northern Norway. *Geochim Cosmochim Acta* 69, 4631-4647.

586 Knies, J., Brookes, S., Schubert, C.J., 2007. Re-assessing the nitrogen signal in continental margin
587 sediments: New insights from the high northern latitudes. *Earth Planet Sc Lett* 253, 471-484.

588 Knies, J., Hald, M., Ebbesen, H., Mann, U., Vogt, C., 2003. A deglacial–middle Holocene record of
589 biogenic sedimentation and paleoproductivity changes from the northern Norwegian continental
590 shelf. *Paleoceanography* 18, 1096.

591 Knies, J., Martinez, P., 2009. Organic matter sedimentation in the western Barents Sea region:
592 Terrestrial and marine contribution based on isotopic composition and organic nitrogen content.
593 *Norw J Geol* 89, 79-89.

594 Knudson, K.P., Hendy, I.L., Neil, H.L., 2011. Re-examining Southern Hemisphere westerly wind
595 behavior: insights from a late Holocene precipitation reconstruction using New Zealand fjord
596 sediments. *Quaternary Sci Rev* 30, 3124-3138.

597 Kristensen, D.K., Sejrup, H.P., Haflidason, H., Berstad, I.M., Mikalsen, G., 2004. Eight-hundred-year
598 temperature variability from the Norwegian continental margin and the North Atlantic thermohaline
599 circulation. *Paleoceanography* 19.

600 Lamy, F., Hebbeln, D., Rohl, U., Wefer, G., 2001. Holocene rainfall variability in southern Chile: a
601 marine record of latitudinal shifts of the Southern Westerlies. *Earth Planet Sc Lett* 185, 369-382.
602 Loring, D.H., 1990. Lithium — a new approach for the granulometric normalization of trace metal
603 data. *Mar Chem* 29, 155-168.
604 Ludwig, W., Probst, J.L., Kempe, S., 1996. Predicting the oceanic input of organic carbon by
605 continental erosion. *Global Biogeochem Cy* 10, 23-41.
606 Martinez, P., Bertrand, P., Shimmield, G.B., Karen, C., Jorissen, F.J., Foster, J., Dignan, M., 1999.
607 Upwelling intensity and ocean productivity changes off Cape Blanc (northwest Africa) during the last
608 70,000 years: geochemical and micropalaeontological evidence. *Mar Geol* 158, 57-74.
609 Mikalsen, G., Sejrup, H.P., Aarseth, I., 2001. Late-Holocene changes in ocean circulation and climate:
610 foraminiferal and isotopic evidence from Sulafjord, western Norway. *Holocene* 11, 437-446.
611 Mil-Homens, M., Vale, C., Raimundo, J., Pereira, P., Brito, P., Caetano, M., 2014. Major factors
612 influencing the elemental composition of surface estuarine sediments: The case of 15 estuaries in
613 Portugal. *Mar Pollut Bull* 84, 135-146.
614 Mitchelson-Jacob, G., Sundby, S., 2001. Eddies of Vestfjorden, Norway. *Cont Shelf Res* 21, 1901-
615 1918.
616 Müller, A., 2011. Potential of rare earth element and Zr-, Be-, U-, Th-, (W-) mineralisations in central
617 northern Nordland - Part 2, NGU Report. Geological Survey of Norway, Trondheim.
618 Munoz, Y.P., Wellner, J.S., 2016. Local controls on sediment accumulation and distribution in a fjord
619 in the West Antarctic Peninsula: implications for palaeoenvironmental interpretations. *Polar Res* 35.
620 Nasuti, A., Roberts, D., Dumais, M.-A., Ofstad, F., Hyvönen, E., Stampolidis, A., 2015. New high-
621 resolution aeromagnetic and radiometric surveys in Finnmark nad North Troms: linking anomaly
622 patterns to bedrock geology and structure. *Norw J Geol* 95, 217-244.
623 Ottesen, D., Rise, L., Knies, J., Olsen, L., Henriksen, S., 2005. The Vestfjorden-Trænedjupet palaeo-ice
624 stream drainage system, mid-Norwegian continental shelf. *Mar Geol* 218, 175-189.
625 Paetzel, M., Dale, T., 2010. Climate proxies for recent fjord sediments in the inner Sognefjord region,
626 western Norway. Geological Society, London, Special Publications 344, 271-288.
627 Pe-Piper, G., Triantafyllidis, S., Piper, D.J.W., 2008. Geochemical identification of clastic sediment
628 provenance from known sources of similar geology: The cretaceous Scotian Basin, Canada. *J*
629 *Sediment Res* 78, 595-607.
630 Petschick, R., Kuhn, G., Gingele, F., 1996. Clay mineral distribution in surface sediments of the South
631 Atlantic: sources, transport, and relation to oceanography. *Mar Geol* 130, 203-229.
632 Rasmussen, A., 1984. Late Weichselian moraine chronology of the Vesterålen islands, North Norway.
633 *Norw J Geol* 64, 193-219.
634 Raymond, P.A., Bauer, J.E., 2001. Riverine export of aged terrestrial organic matter to the North
635 Atlantic Ocean. *Nature* 409, 497-500.
636 Ruddiman, W.F., McIntyre, A., 1981. The North Atlantic Ocean during the last deglaciation.
637 *Palaeogeography, Palaeoclimatology, Palaeoecology* 35, 145-214.
638 Sargent, J.R., Hopkins, C.C.E., Seiring, J.V., Youngson, A., 1983. Partial characterization of organic
639 material in surface sediments from Balsfjorden, northern Norway, in relation to its origin and
640 nutritional value for sediment-ingesting animals. *Mar Biol* 76, 87-94.
641 Schlüter, M., Sauter, E., 2000. Biogenic silica cycle in surface sediments of the Greenland Sea. *Journal*
642 *of Marine Systems* 23, 333-342.
643 Schneider, R.R., Schulz, H.D., Hensen, C., 2006. Marine Carbonates: Their Formation and Destruction,
644 in: Schulz, H.D., Zabel, M. (Eds.), *Marine Geochemistry*. Springer Berlin Heidelberg, Berlin,
645 Heidelberg, pp. 311-337.
646 Sepúlveda, J., Pantoja, S., Hughen, K.A., 2011. Sources and distribution of organic matter in northern
647 Patagonia fjords, Chile (~44-47°S): A multi-tracer approach for carbon cycling assessment. *Cont Shelf*
648 *Res* 31, 315-329.

649 Shimmiel, G.B., 1992. Can sediment geochemistry record changes in coastal upwelling
650 palaeoproductivity? Evidence from northwest Africa and the Arabian Sea. Geological Society,
651 London, Special Publications 64, 29-46.

652 Silva, N., Vargas, C.A., Prego, R., 2011. Land–ocean distribution of allochthonous organic matter in
653 surface sediments of the Chiloé and Aysén interior seas (Chilean Northern Patagonia). *Cont Shelf Res*
654 *31*, 330-339.

655 Skei, J., 1983. Why sedimentologists are interested in Fjords. *Sediment Geol* *36*, 75-80.

656 Smith, R.W., Bianchi, T.S., Allison, M., Savage, C., Galy, V., 2015. High rates of organic carbon burial in
657 fjord sediments globally. *Nat Geosci* *8*, 450-U446.

658 St-Onge, G., Hillaire-Marcel, C., 2001. Isotopic constraints of sedimentary inputs and organic carbon
659 burial rates in the Saguenay Fjord, Quebec. *Mar Geol* *176*, 1-22.

660 Stein, R., MacDonald, R.W., 2004. *The Organic Carbon Cycle in the Arctic Ocean*. Springer, Berlin
661 Heidelberg.

662 Sundby, S., 1982. Vestfjordundersøkelsene 1978. 1. Ferskvannsbudsjett og vindforhold
663 (Investigations in Vestfjorden 1978. 1. Fresh water budget and wind conditions), Fisken og havet.
664 Havforskningsinstituttet, pp. 1-30.

665 Sundby, S., Solemdal, P., 1984. The egg production of Arcto-Norwegian cod (*Gadus morhua* L.) in the
666 Lofoten area estimated by egg surveys, The proceedings of the Soviet-Norwegian symposium on:
667 Reproduction and recruitment of Arctic cod. PINRO-IMR Symposium, Leningrad, pp. 113-135.

668 Syvitski, J.P.M., 1989. On the deposition of sediment within glacier-influenced fjords: Oceanographic
669 controls. *Mar Geol* *85*, 301-329.

670 Syvitski, J.P.M., Burrell, D.C., Skei, J.M., 1987. *Fjords: Processes and Products*. Springer-Verlag, New
671 York.

672 Velde, B., 1995. *Origin and Mineralogy of Clays: Clays and the Environment*. Springer-Verlag Berlin
673 Heidelberg.

674 Vogt, C., Knies, J., 2009. Sediment pathways in the western Barents Sea inferred from clay mineral
675 assemblages in surface sediments. *Norw J Geol* *89*, 41-55.

676 Vogt, C., Lauterjung, J., Fischer, R.X., 2002. Investigation of the Clay Fraction (<2µm) of the Clay
677 Minerals Society Reference Clays. *Clays and Clay Minerals* *50*, 388-400.

678 Wehrmann, L.M., Formolo, M.J., Owens, J.D., Raiswell, R., Ferdelman, T.G., Riedinger, N., Lyons,
679 T.W., 2014. Iron and manganese speciation and cycling in glacially influenced high-latitude fjord
680 sediments (West Spitsbergen, Svalbard): Evidence for a benthic recycling-transport mechanism.
681 *Geochim Cosmochim Acta* *141*, 628-655.

682 White, A.F., Blum, A.E., 1995. Effects of Climate on Chemical-Weathering in Watersheds. *Geochim*
683 *Cosmochim Acta* *59*, 1729-1747.

684 Wilson, M.J., 2004. Weathering of the primary rock-forming minerals: processes, products and rates.
685 *Clay Miner* *39*, 233-266.

686 Winkelmann, D., Knies, J., 2005. Recent distribution and accumulation of organic carbon on the
687 continental margin west off Spitsbergen. *Geochem Geophys Geosy* *6*.

688 Yarincik, K.M., Murray, R.W., Peterson, L.C., 2000. Climatically sensitive eolian and hemipelagic
689 deposition in the Cariaco Basin, Venezuela, over the past 578,000 years: Results from Al/Ti and K/Al.
690 *Paleoceanography* *15*, 210-228.

691 Zabel, M., Schneider, R.R., Wagner, T., Adegbe, A.T., de Vries, U., Kolonic, S., 2001. Late Quaternary
692 climate changes in central Africa as inferred from terrigenous input to the Niger fan. *Quaternary Res*
693 *56*, 207-217.

694 Zamelczyk, K., Rasmussen, T.L., Husum, K., Godtlielsen, F., Hald, M., 2014. Surface water conditions
695 and calcium carbonate preservation in the Fram Strait during marine isotope stage 2, 28.8–15.4 kyr.
696 *Paleoceanography* *29*, 1-12.

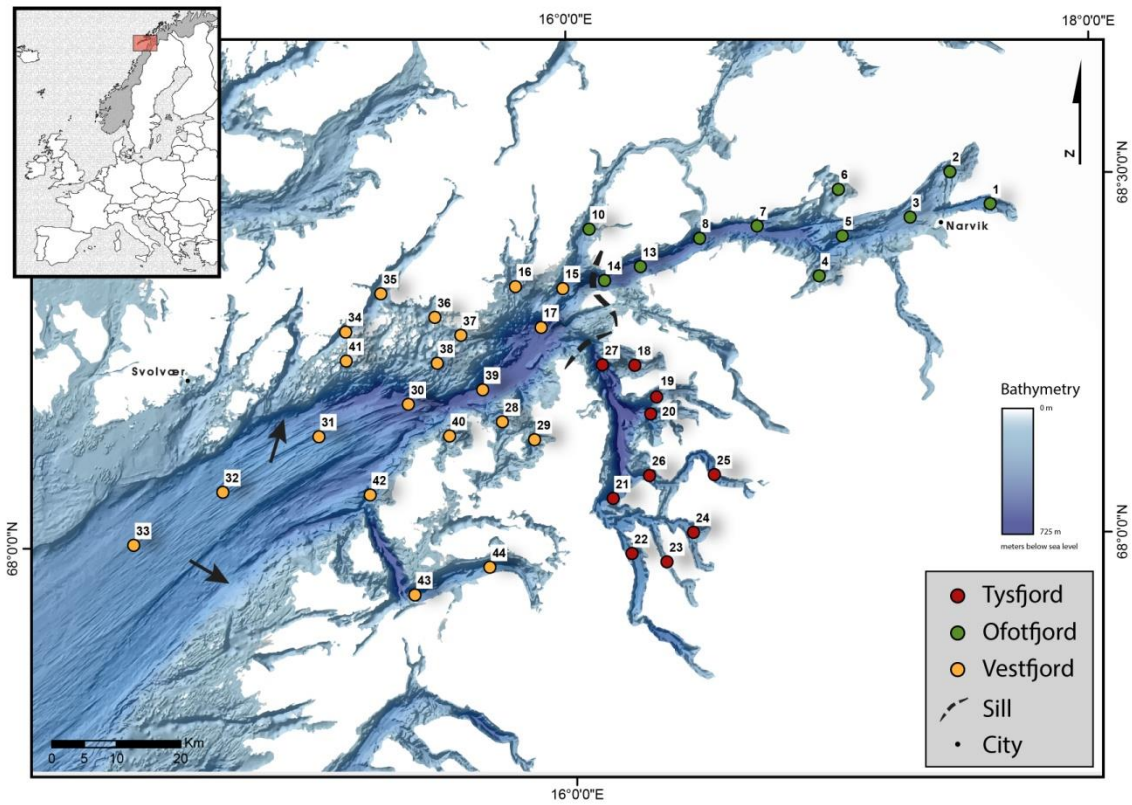
697

698

699 **Figures**

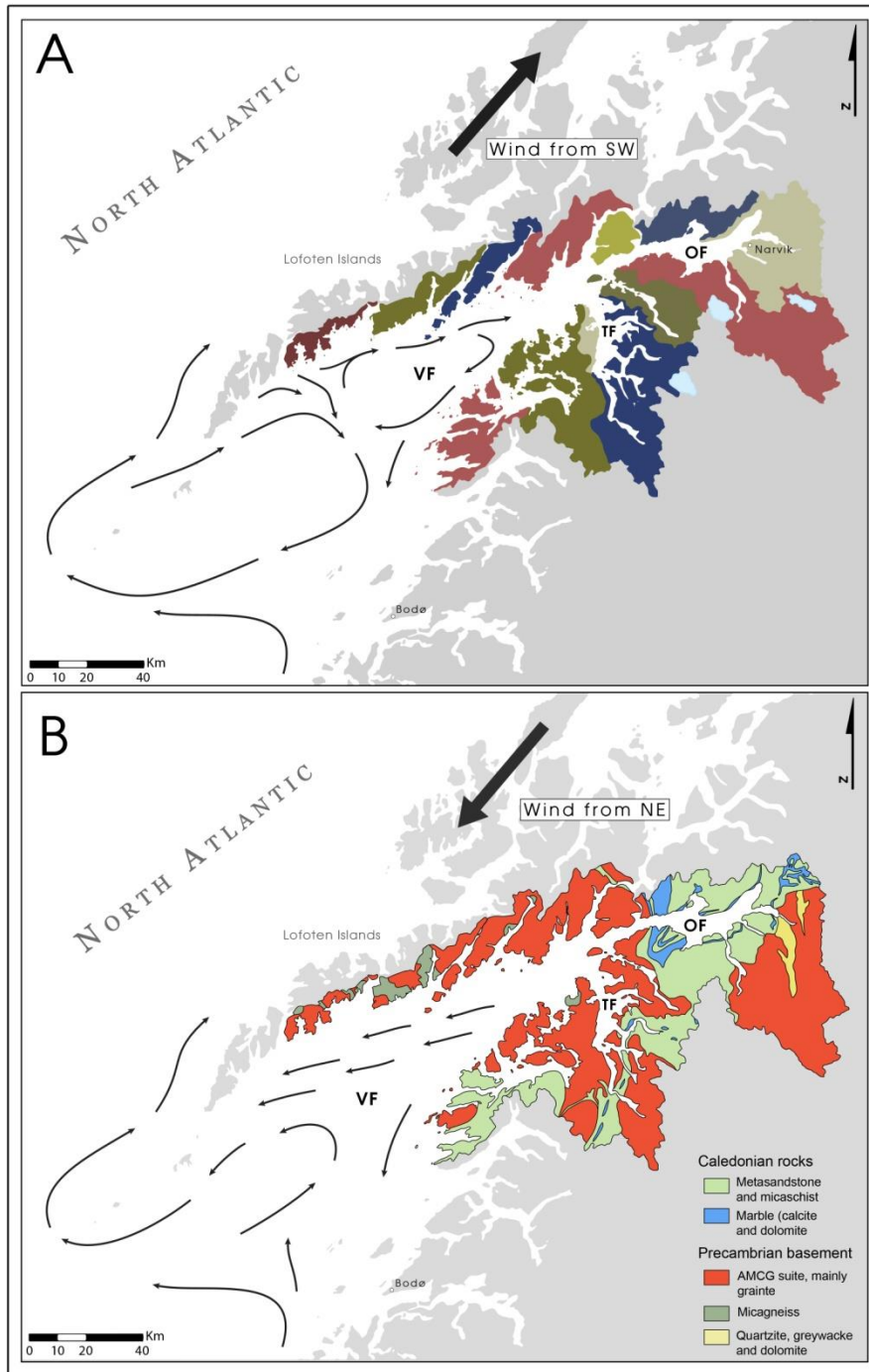
700

701



702

703 **Fig. 1:** Location of the study area in northern Norway (upper left inlet). Map of the Vest-,
704 Ofot- and Tysfjord showing the bathymetry (from mareano.no) and sampling positions of
705 each fjord (ES-1). Broken black line indicates the sill between the three fjords. Black arrows
706 indicate the up to 300 m high side-edge between the deeper Vestfjord basin and its
707 shallower coastal areas.



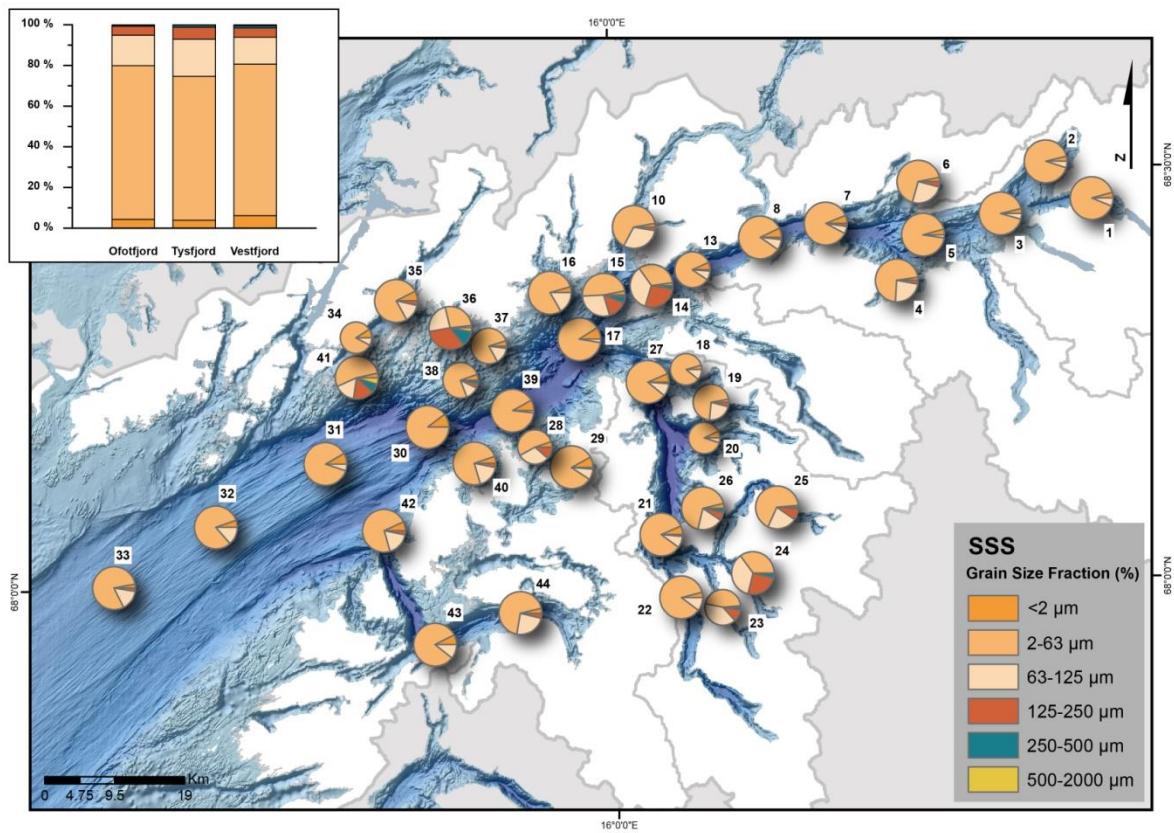
708

709 **Fig. 2:** The Vestfjord (VF), Ofotfjord (OF) and Tysfjord (TY) are the three main fjords of a
 710 complex fjord system between the Norwegian mainland and the Lofoten archipelago in
 711 northern Norway. **A)** Total catchment area of the three fjords. Each coloured field
 712 represents a sub-drainage basin. The three main glaciers present in the drainage area today
 713 are indicated by white fields in the south of the Ofot- and Tysfjord. Additionally, black
 714 arrows indicate the surface circulation pattern during SW winds. **B)** Simplified geological
 715 map of the study area and surface circulation during NE winds (black arrows).

716

717

718



719

720 **Fig. 3:** Grain size distribution in the Vestfjord, Ofofjord and Tysfjord surface sediment
721 sample (SSS) and average grain size of each fjord (bar chart, upper left). To prevent the pie
722 diagrams to overlap they vary in sizes.

723

724

725

726

727

728

729

730

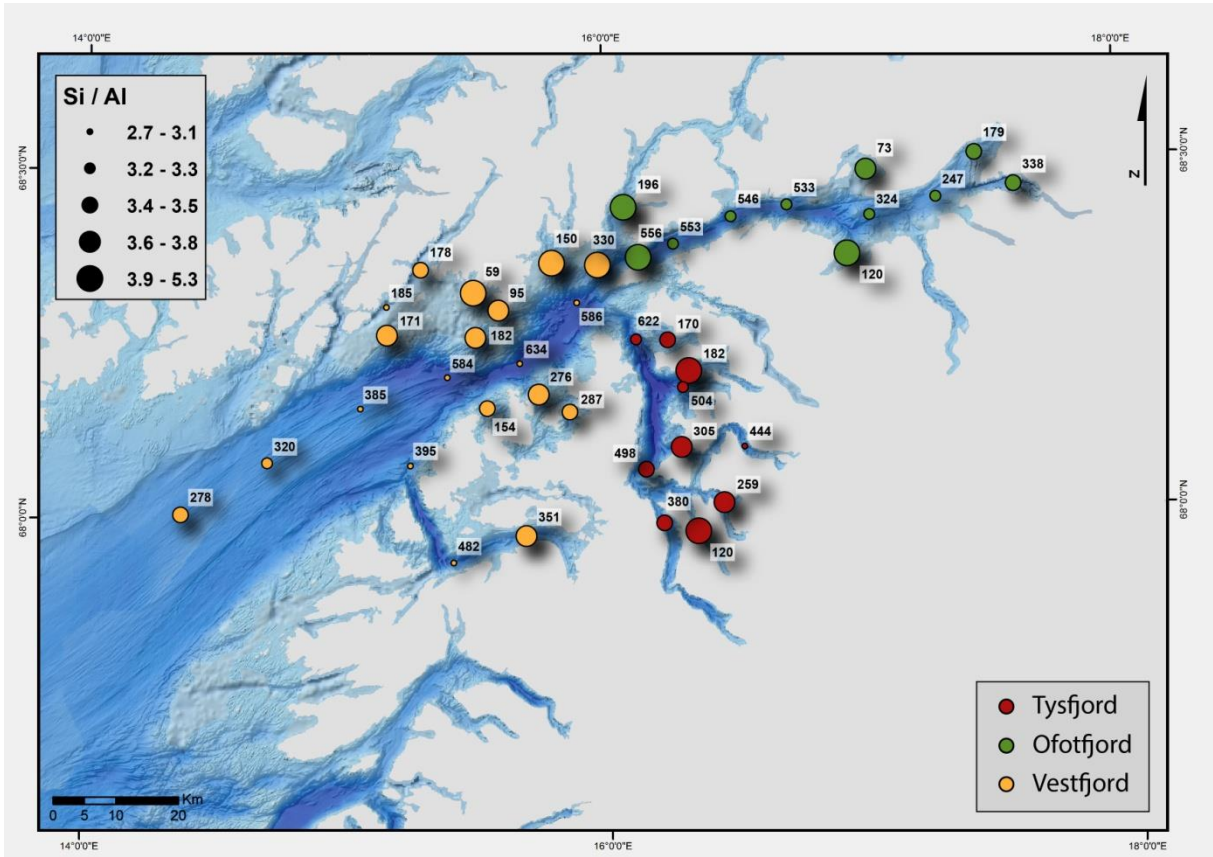
731

732

733

734

735



736

737 **Fig. 4:** Water depth and spatial distribution of Si/Al of the surface sediments samples from
738 the Vestfjord (yellow), Ofofjord (green) and Tysfjord (red).

739

740

741

742

743

744

745

746

747

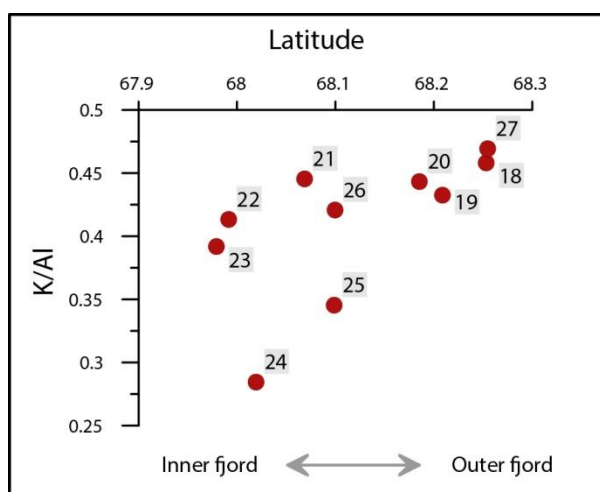
748

749

750

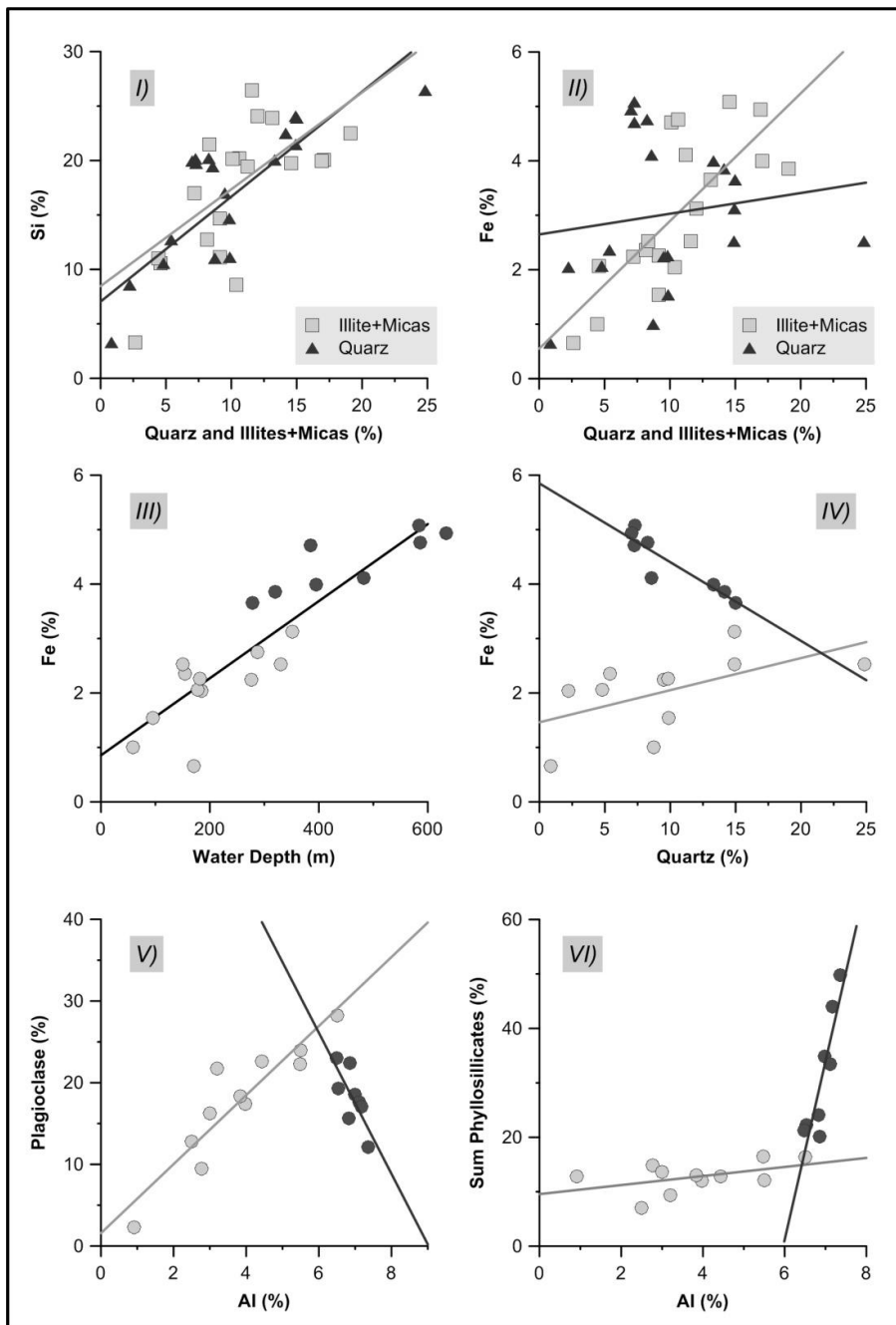
751

752



753

754 **Fig. 5:** K/Al in the Tysfjord surface sediment samples with station numbers. K/Al reveal a
755 clear inside outside trend with highest values at the entrance of the fjord.

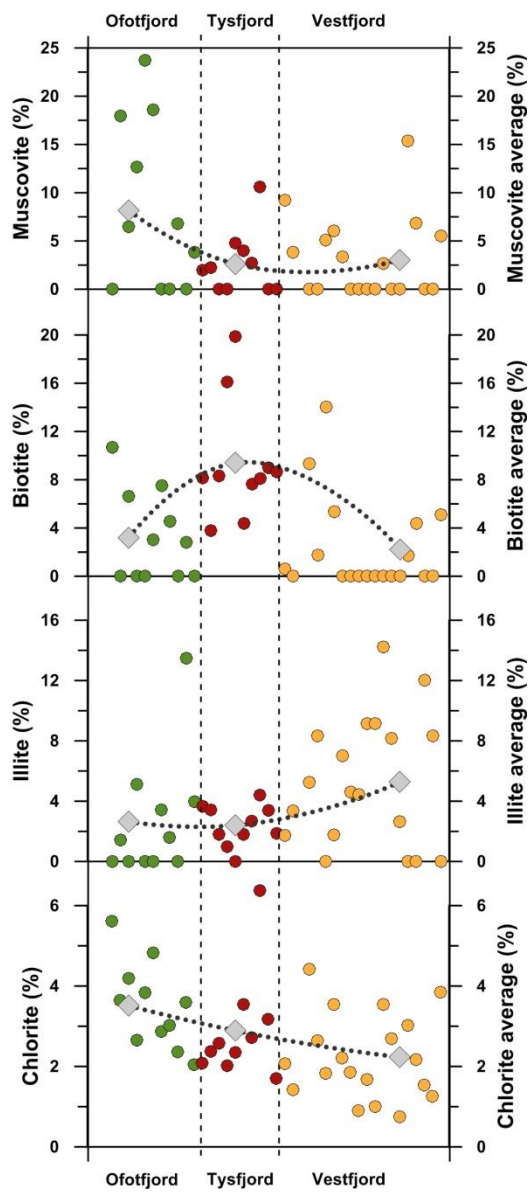


756

757 **Fig. 6:** (I) Considering all samples from the Vestfjord Si correlates with quartz ($r = 0.8$) and
 758 the sum of illites and micas ($r = 0.7$). (II) Fe correlates with the sum of illites and micas
 759 ($r = 0.8$) but not with quartz ($r = 0.2$). (III) Fe is strongly related to the water depth of the
 760 sample ($r = 0.9$). Light grey points: samples from the shelf and sill (stations 15; 16; 28; 29;
 761 34–38; 40; 41; 44, Fig. 1), dark grey points: samples from the deep basin (stations 17; 30–33;
 762 39; 42; 43, Fig. 1). (IV) Fe and quartz are positive correlated on the shelf areas ($r = 0.6$) and
 763 negative in the deeper and outer fjord basins ($r = -0.9$). (V) Al versus plagioclase reveals a
 764 clear positive correlation ($r = 0.9$) for the shelf and sill sediment samples and a clear
 765 negative correlation ($r = -0.8$) for the samples from the deeper Vestfjord basin. (VII) Al
 766 versus the sum of phyllosilicates shows an increase of the Pearson correlation coefficient
 767 from $r = 0.4$ at the shallow parts to $r = 0.9$ in the deeper fjord areas.

768

769



770

771 **Fig.7:** Muscovite, biotite, illite and chlorite concentrations (%) in the surface sediments
772 samples from the Ofotfjord (green), Tysfjord (red) and Vestfjord (yellow). Average content is
773 indicated by grey diamonds.

774

775

776

777

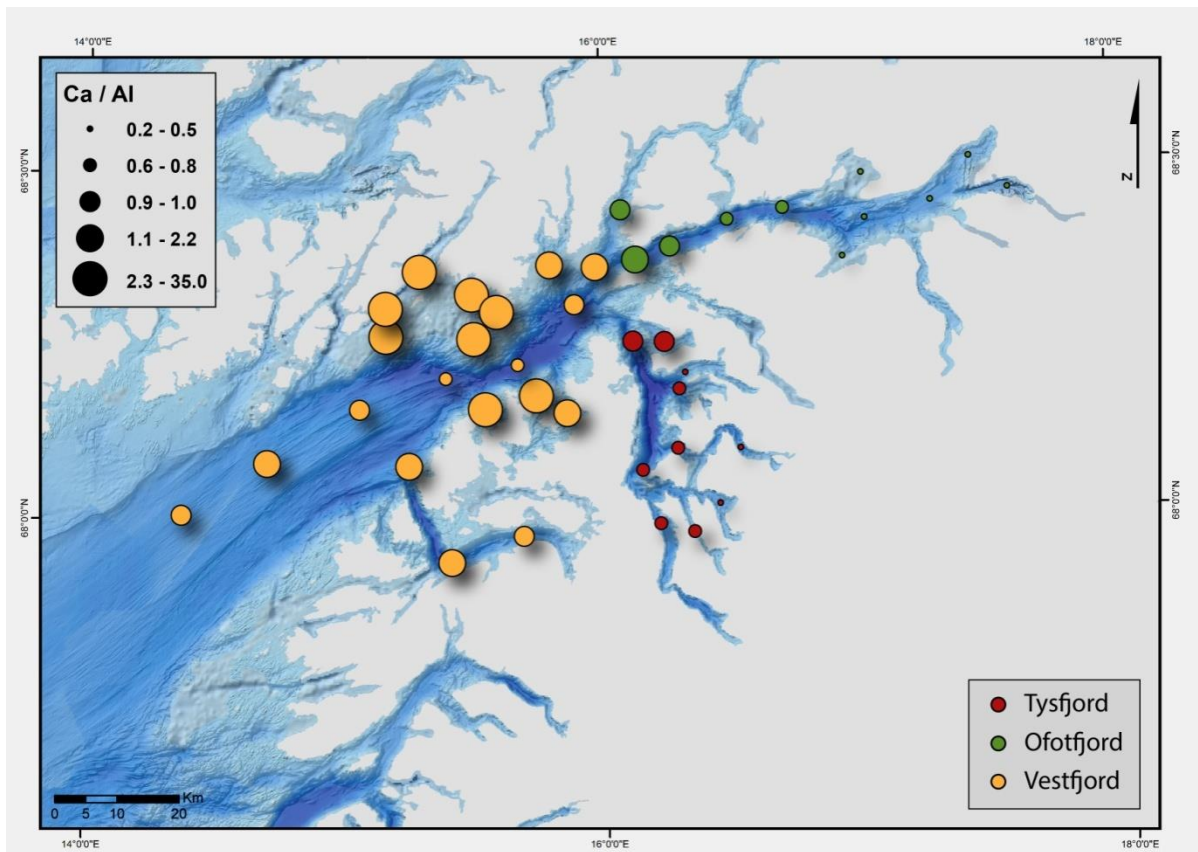
778

779

780

781

782



783

784 **Fig. 8:** Ca/Al distribution in the surface sediments of the Ofotfjord (green), Tysfjord (red)
785 and Vestfjord (yellow). Highest values are found close to the sill and at the shallow shore
786 areas of in the NW and SE of the Vestfjord.

787

788